Sensors **2008**, *8*, 4774-4785; DOI: 10.3390/s8084774

OPEN ACCESS

sensors

ISSN 1424-8220

www.mdpi.org/sensors

Article

CO_2 Selective Potentiometric Sensor in Thick-film Technology

Kathy Sahner [1,*], Anne Schulz [1], Jaroslaw Kita [1], Rotraut Merkle [2], Joachim Maier [2] and Ralf Moos [1]

1 Functional Materials Laboratory, University of Bayreuth, 95440 Bayreuth, Germany

2 Max-Planck-Institut für Festkörperforschung, Stuttgart, Germany

* Author to whom correspondence should be addressed; E-Mail: Functional.Materials@Uni-Bayreuth.de (K. Sahner); Tel.: +49-921-557401; Fax: +49-921-557405

Received: 2 July 2008; in revised form: 8 August 2008 / Accepted: 8 August 2008 / Published: 19 August 2008

Abstract: A potentiometric sensor device based on screen-printed Nasicon films was investigated. In order to transfer the promising sensor concept of an open sodium titanate reference to thick film technology, "sodium-rich" and "sodium-poor" formulations were compared. While the "sodium-rich" composition was found to react with the ion conducting Nasicon during thermal treatment, the "sodium-poor" reference mixture was identified as an appropriate reference composition. Screen-printed sensor devices were prepared and tested with respect to CO_2 response, reproducibility, and cross-interference of oxygen. Excellent agreement with the theory was observed. With the integration of a screen-printed heater, sensor elements were operated actively heated in a cold gas stream.

Keywords: Ion conductor, solid-state reference, electrochemical sensor.

1. Introduction

Due to its strong impact as a greenhouse gas, monitoring of CO_2 emissions has become crucial. Although optical detection of CO_2 using infrared radiation is very exact, a more cost-effective method capable of also working in harsh and dirty environments is needed. To meet these requirements, several potentiometric sensor devices based on electrochemical cells with sodium conducting solid electrolytes such as β''-Al_2O_3 or $Na_{1+x}Zr_2P_{3-x}Si_xO_{12}$ (Nasicon, $0 \leq x \leq 3$) have been investigated (for a detailed review, cf. [1]). Corresponding to a "type III" electrochemical gas sensor [2], these sensor devices rely on the presence of an auxiliary phase such as sodium or barium carbonate, which is deposited at the working electrode and interacts with CO_2. As the counter or reference electrode, gold or platinum are

often used. Despite their frequent use, it has to be emphasized that such pure metal electrodes are not able to provide a thermodynamically well-defined chemical potential of sodium.

In many of these electrochemical cells, the electrolyte material forms a thin ceramic pellet or tube [3 - 8]. More recently, sensor designs based on screen-printed or dip-coated ion-conducting films have been reported [9 -14].

As a major drawback, the devices relying *only* on a carbonate auxiliary phase exhibit a pronounced cross-sensitivity towards oxygen, poor reproducibility between single sensor elements, and poor long-term stability. As an alternative approach, sodium titanate ($Na_2Ti_6O_{13}/Na_2Ti_3O_7$) or sodium titanate/titania ($Na_2Ti_6O_{13}/TiO_2$) mixtures were proposed as a reference system [15 - 17]. These two phase mixture systems provided a thermodynamically well-defined signal based on an oxygen-independent overall reaction as shown below.

sensing electrode: $Na_2CO_3 \leftrightarrow 2\ Na^+ + CO_2 + 0.5\ O_2 + 2\ e^-$

reference 1: $2\ Na^+ + Na_2Ti_6O_{13} + 0.5\ O_2 + 2\ e^- \leftrightarrow 2\ Na_2Ti_3O_7$ (1)

overall reaction: $Na_2CO_3 + Na_2Ti_6O_{13} \leftrightarrow CO_2 + 2\ Na_2Ti_3O_7$

or reference 2: $2\ Na^+ + 6\ TiO_2 + 0.5\ O_2 + 2\ e^- \leftrightarrow Na_2Ti_6O_{13}$ (2)

overall reaction: $Na_2CO_3 + 6\ TiO_2 \leftrightarrow CO_2 + Na_2Ti_6O_{13}$

As derived in detail in [15], the resulting electromotive force *emf* of these cells is related to the chemical potential difference of the sodium ions at the electrodes according to Eq. 3.

$$emf = -\frac{1}{F}\left(\mu_{Na^+}^{reference} - \mu_{Na^+}^{carbonate}\right) \tag{3}$$

where F denotes the Faraday constant, and $\mu_{Na^+}^{i}$ is the chemical potential of the sodium ions at the reference and the working electrode, respectively.

Since both $\mu_{Na^+}^{reference}$ and $\mu_{Na^+}^{carbonate}$ are well-defined within this set-up, the *emf* of these cells was shown to depend solely on the carbon dioxide partial pressure pCO_2 and on the operating temperature T of the device [15]. As a consequence, simultaneous knowledge of the sensor temperature and the geometry-independent parameter *emf* enables one to precisely determine pCO_2. The fact that the *emf* is defined thermodynamically also implies the absence of long-term drift effects.

Since the cells discussed in [15] were prepared from bulky ceramic pellets, their usefulness in real-world applications was limited. In particular, homogeneous heating of such cells can only be achieved in a furnace, and the integration of a temperature sensor to precisely monitor the operating temperature is not straight-forward. It is therefore highly desirable to transfer the present promising sensor concept to thick-film technology, which provides a basis for miniaturization and integration of further functionalities such as heater and temperature sensor with a single sensor chip.

In this contribution, we report results obtained on long-term stable CO_2 sensors with a sodium titanate reference prepared entirely via a cost-effective screen-printing technique. In a detailed study,

the most appropriate reference system was identified. In addition to the basic sensor characteristics, the devices were tested with respect to cross-interference of oxygen and long-term stability.

2. Experimental

2.1 Precursor preparation

All ceramic precursor powders were prepared by a conventional mixed-oxide route. To obtain the *Nasicon* composition $Na_{1+x}Zr_2P_{3-x}Si_xO_{12}$ with x = 2.2, Na_2CO_3 (Merck), $NH_4H_2PO_4$ (VWR), SiO_2 (VWR), and ZrO_2 (AlfaAesar) were mixed in stoichiometric amounts in a ball mill and calcined at 1050 °C for 12 h.

In the case of the *sodium titanate compositions* $Na_2Ti_6O_{13}$ and $Na_2Ti_3O_7$, Na_2CO_3 (p.a., VWR) and TiO_2 (anatase, Sigma Aldrich) served as precursors. The corresponding Na_2CO_3/TiO_2 powder mixtures (molar ratio 1:3 and 1:6, respectively) were mixed for 4 h in a ball mill and then calcined at 900 °C for 6 h.

Figure 1 presents the XRD patterns of the as-prepared Nasicon, $Na_2Ti_3O_7$, and $Na_2Ti_6O_{13}$ powders (Philips PW 3710, Cu-K_α radiation, Bragg-Brentano geometry). While both sodium titanate compositions were found to be phase-pure, some impurity peaks attributed to ZrO_2 (symbol ◊) and $Na_2ZrSi_2O_7$ (symbol □) were observed within the Nasicon.

Figure 1. X-ray diffractograms of the as-prepared $Na_2Ti_3O_7$, $Na_2Ti_6O_{13}$ and Nasicon powder.

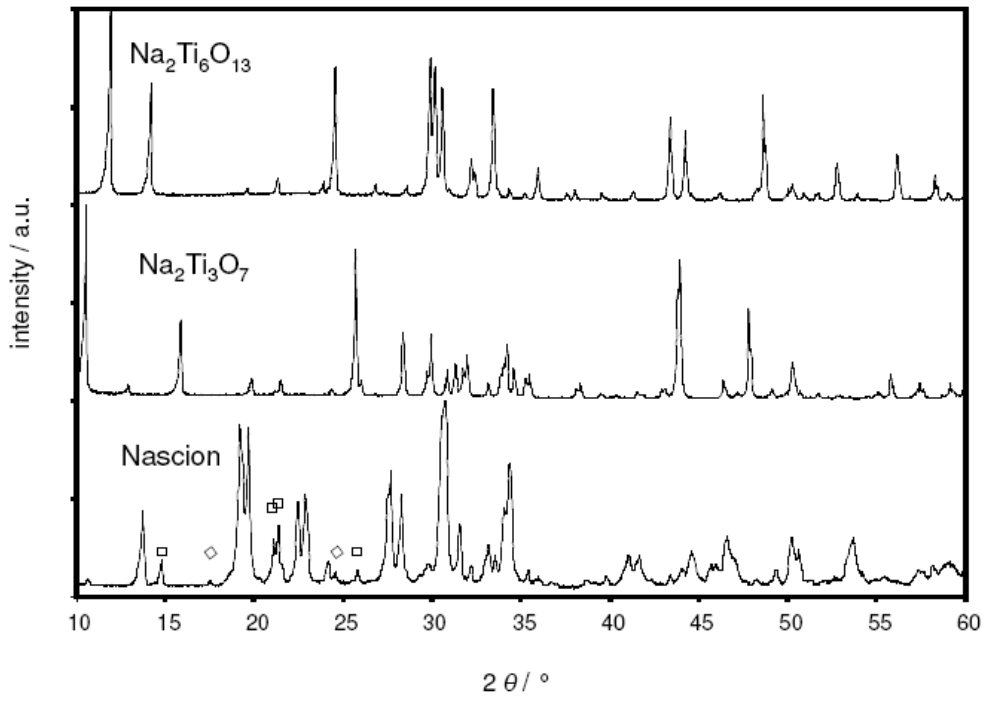

Two *reference compositions* were tested in the present study. The "sodium-rich" reference consisted of a $Na_2Ti_6O_{13}/Na_2Ti_3O_7$ (molar ratio: 1:1) mixture, while the "sodium-poor" composition was formed by mixing $Na_2Ti_6O_{13}$ and TiO_2 powder with a molar ratio of 1:1.

An eutectic mixture of $Na_2CO_3/BaCO_3$ with a molar ratio of 1.72:1 served as the *auxiliary carbonate phase*. Prior to mixing, both precursor powders [Na_2CO_3 (p.a., VWR) and $BaCO_3$ (Selectipur, Merck)] were dried at 450 °C. The carbonate mixture was heated at 5 K/min to 720 °C, a temperature above the melting point. The melt was retrieved from the furnace and quenched onto a brass plate. The as-obtained material was ground in a mortar.

In order to prepare screen-printable pastes, each of the as-prepared powders was sieved (< 200 µm) and mixed with a thixotropic organic binder to form a homogeneous paste.

2.2 Sensor preparation

The sensor set-up is shown diagrammatically in Figure 2. On top of a bare alumina substrate, a Nasicon layer was screen-printed and fired at 1050 °C for 5 h. Then, either the $Na_2Ti_3O_7$/ $Na_2Ti_6O_{13}$ or the $Na_2Ti_6O_{13}/TiO_2$ reference was printed on one side of the Nasicon film and fired at 950 °C for 5 h. Two gold grid electrodes were printed according to Figure 2 (firing at 850 °C). Finally, the sensitive $Na_2CO_3/BaCO_3$ mixture was painted on top of one gold grid and heat treated at 600 °C.

Figure 2. Diagrammatical representation of the sensor cross section.

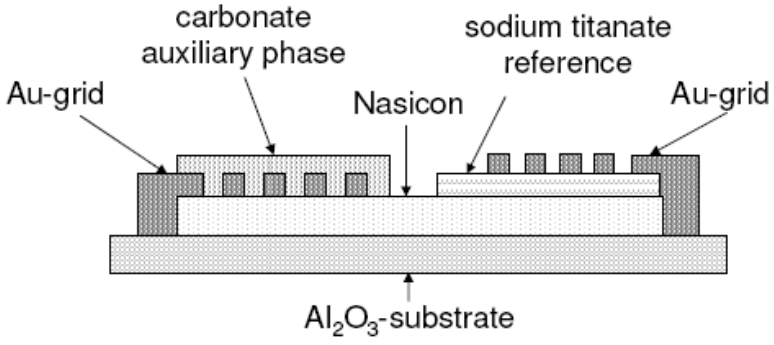

2.3. XRD study

In order to study compatibility between the reference materials and the solid electrolyte, XRD studies were conducted in the 2θ range from 10 ° to 90 °. Two samples were prepared by mixing either 0.75 g $Na_2Ti_3O_7$ with 1 g Nasicon or 0.6 g $Na_2Ti_6O_{13}$ with 1 g Nasicon, respectively. While one part of these mixtures was studied directly by XRD, one part was heat-treated at 950 °C for 5 h using the sintering profile of the reference thick films.

2.4 Sensor tests

For tests of the sensor performance, a custom-build test bench similar to the one described in [18] for hydrocarbon sensing was used. The sensors were inserted into a tube furnace and heated to their operating temperature either with the furnace or actively via the platinum heater (see below). The total gas flow was adjusted to 200 sccm/min with dry air serving as the carrier gas. The carbon dioxide partial pressure was varied in the range of 0.4 mbar to 45 mbar by diluting pure CO_2 gas with dry air

using mass flow controllers. The actual CO_2 concentration was monitored by an FTIR (Antaris, ThermoElectron) located downstream the sensor chamber. The *emf* output of the sensor element was monitored using a digital multimeter (Keithley 2700).

3. Results and Discussion

3.1 Sodium-rich reference

In an initial test series, sensor samples with the sodium-rich reference composition $Na_2Ti_3O_7/Na_2Ti_6O_{13}$ were measured. In Figure 3, the *emf* trace at 500 °C upon CO_2 exposure is shown exemplarily. The sensor device presented a stable and perfectly reversible response. An additional variation of the oxygen partial pressure from 0.15 bar to 0.27 bar indicated no cross sensitivity of the sensor to this gas as expected from the literature.

Figure 3. Sensor response towards pCO_2 and oxygen cross-interference test at 500 °C on a sensor device with the sodium-rich reference. **Top:** partial pressure of the test gases. **Bottom:** Sensor signal.

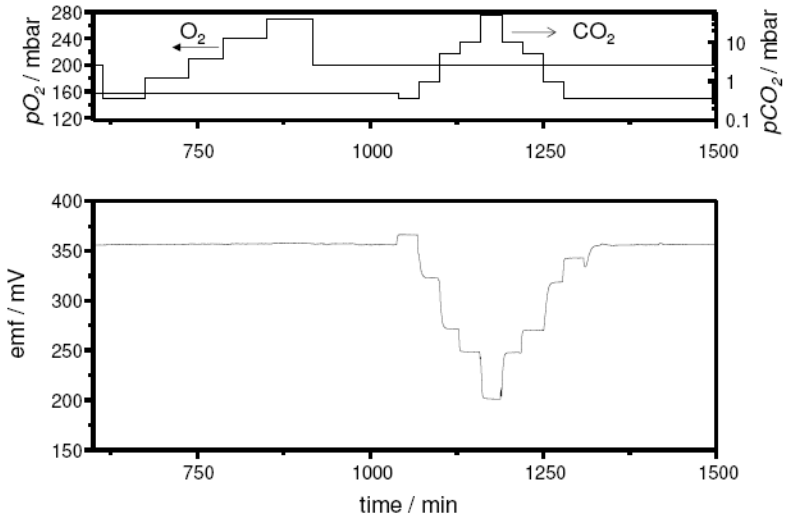

To evaluate the sensor performance, the semilogarithmic representation $emf = f(\log(pCO_2))$ was used. With the slope of this plot, the electron transfer number n of the electrochemical reaction can be calculated according to the Nernst equation (Eq. 4)

$$emf = E_0 - \frac{RT}{nF}\ln\left(\frac{pCO_2}{p^0}\right) = E_0 - \underbrace{\frac{RT\ln 10}{nF}}_{slope}\log\left(\frac{pCO_2}{p^0}\right) \quad (4)$$

with p^0 = 1013 mbar.

As known from the cell reactions (1) and (2), the theoretical electron transfer number equals 2. With the present sensor set up, values of 2.14 ± 0.06 (total of 4 specimens, each measured 3 times at 500 °C) and 2.12 ± 0.06 (total of 4 specimens at 600 °C) were determined.

In spite of the promising sensor characteristics, the thick film devices with the sodium-rich reference presented a much higher *emf* reading than expected from the thermodynamic calculations and experimental results on the pellet-type sensor discussed in [15]. In Figure 4, this deviation between pellet-type sensor (open symbols) and the corresponding thick-film device measured in the present study (closed symbols) is presented. In this case, the temperature-corrected form of the Nernst equation (Eq. 4) was used to compare the experimental results directly with the values expected from theory.

$$\frac{emf - E_0}{T} = -\frac{R}{2F}\ln\left(\frac{pCO_2}{p^0}\right) \tag{4a}$$

The required temperature-dependent values for E_0, i.e. the cell *emf* at $pCO_2 = p^0 = 1013$ mbar, were taken from the literature [15].

Figure 4. Comparison between the experimental results of the thick-film sensor with the sodium-rich reference and the results expected from theory. For details see text.

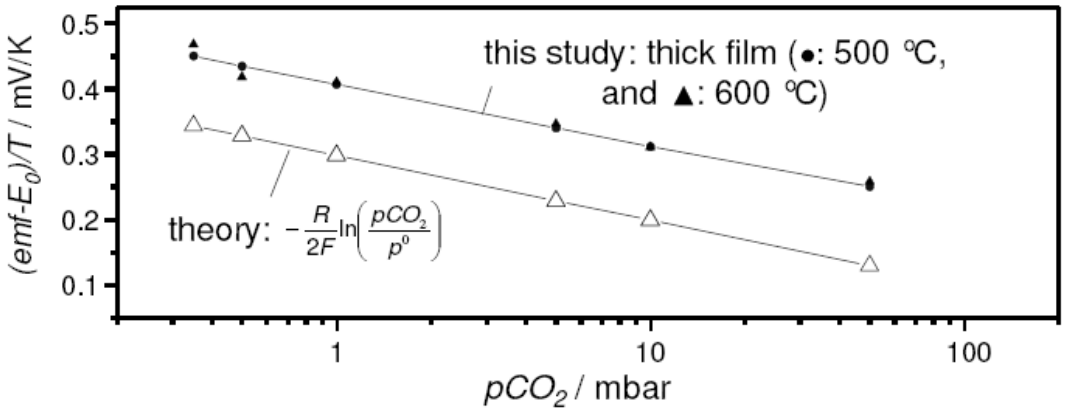

In a supplementary XRD study, the deviation from the theoretical *emf* was attributed to a parasitic reaction between the Nasicon electrolyte and the $Na_2Ti_3O_7$ phase. Figure 5a compares two XRD diagrams obtained from a Nasicon/$Na_2Ti_3O_7$ powder mixture prior (bottom) and after (top) heat treatment at 950 °C, i.e., the sintering temperature of the sodium titanate reference film. For the sake of clarity, only the 2 θ range from 10° to 60° is shown. In the X-ray diffractogram of the untreated powder mixtures, the peaks from both the Nasicon and the titanate phase were identified. In addition, some impurity peaks were found, which were attributed to ZrO_2 und $Na_2ZrSi_2O_7$. These impurities were also present in the Nasicon precursor powder (cf. Figure 1).

The XRD pattern after thermal treatment indicated a thermally activated reaction between the Nasicon and the titanate. The characteristic peaks of $Na_2Ti_3O_7$ (symbol ○ in the bottom figure) are almost completely replaced by the sodium-poor $Na_2Ti_6O_{13}$ phase (symbol Δ). In addition, changes in the Nasicon pattern are observed, e.g., the double peak at 19° is reduced to one broadened peak. This might be attributed to a compositional and structural change of the sodium ion conductor from Nasicon to $Na_4Zr_3Si_3O_{12}$. As an additional phase, Na_3PO_4 is found (symbol □).

While the reactivity between Nasicon and $Na_2Ti_3O_7$ is irrelevant in the case of the separately sintered pellets discussed in [15], it is detrimental for thick film layers that are heat-treated simultaneously. During sintering of the reference electrode, most of the $Na_2Ti_3O_7$ phase reacts with the adjacent Nasicon layer. Due to the different phase composition of the reference electrode mixture its sodium ion activity decreases. As a consequence, the *emf* value of the cell, which is given by the difference of the chemical potentials of sodium ions at each electrode (Eq. 3), is expected to increase.

Figure 5. XRD pattern of Nasicon/$Na_2Ti_3O_7$ and Nasicon/$Na_2Ti_6O_{13}$ powder mixtures.
(a) Nasicon/$Na_2Ti_3O_7$ mixtures before (bottom) and after (top) thermal treatment at 950 °C, respectively. Only some of the characteristic peaks of the $Na_2Ti_3O_7$ are highlighted (symbol ○), which are replaced by the sodium-poor $Na_2Ti_6O_{13}$ phase (symbol Δ) after the thermal treatment. For details see text.
(b) Nasicon/$Na_2Ti_6O_{13}$ mixtures before (bottom) and after (top) thermal treatment at 950 °C, respectively.

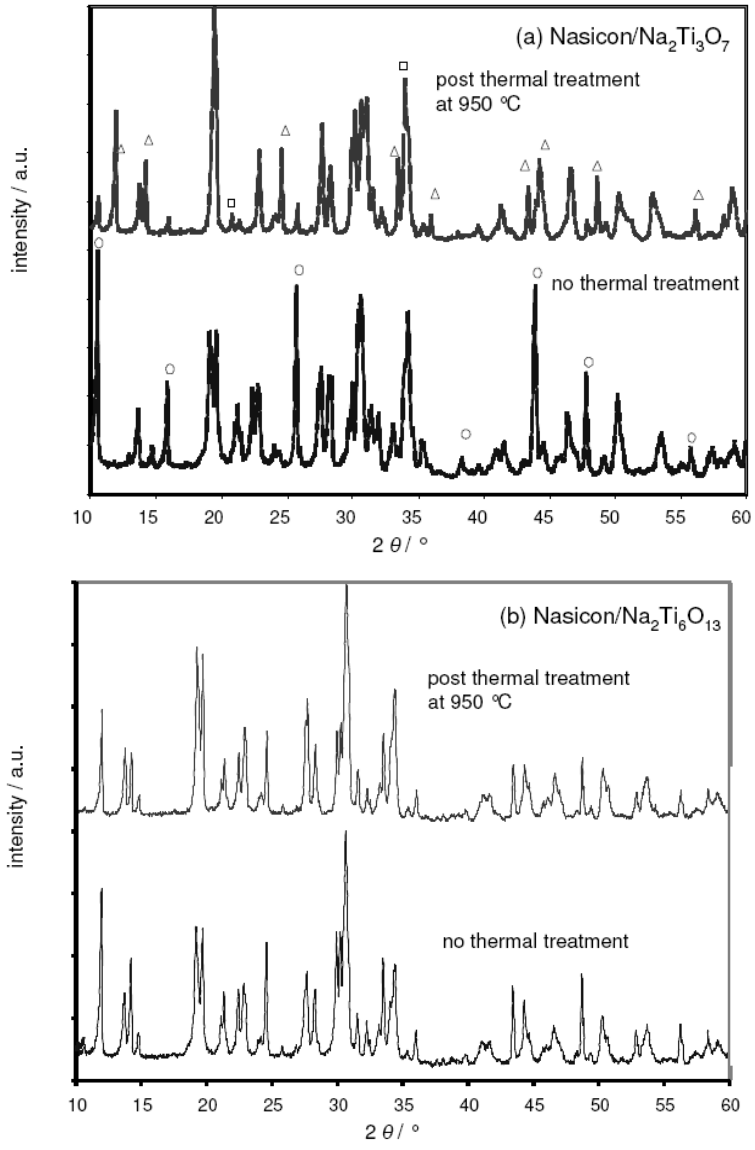

3.2 Sodium-poor reference

In contrast to $Na_2Ti_3O_7$, XRD studies on Nasicon/$Na_2Ti_6O_{13}$ mixtures yielded no evidence for parasitic reactions at 950 °C. Identical XRD patterns were observed prior and after thermal treatment (Figure 5b; no new peaks, only some minor changes in peak intensities appear). The sodium-poor reference composition $Na_2Ti_6O_{13}/TiO_2$ was thus identified as a more promising candidate for thick-film devices.

Figure 6 exemplarily presents the sensitivity plots of a corresponding sensor element. The device was measured several times at three temperatures. In contrast to the sensor devices discussed above, the measured *emf* values (symbols) were found to agree well with the results reported in the literature (lines). Again, Nernstian behavior with an electron transfer number of 1.9 was found. The reproducibility of the measurements is remarkable. In Figure 6, one can hardly distinguish the different runs at 575 °C

Figure 6. *emf* Sensor characteristics of a thick-film device with the sodium-poor reference composition. Operating temperature as indicated. For comparison, data reported in the literature for a pellet-like sensor [15] were included.

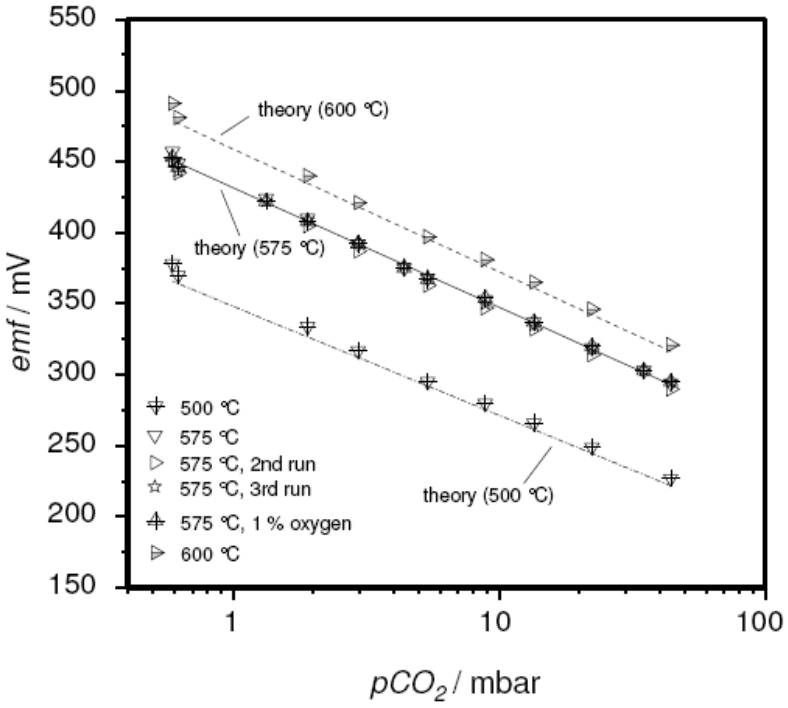

To ensure the reproducibility of the sensor concept, three sensor devices were prepared and measured at various temperatures. The results are summarized in Figure 7. As before (cf. Figure 4), the very sensitive representation:

$$\frac{emf - E_0}{T} = -\frac{R}{2F}\ln\left(\frac{pCO_2}{p^0}\right)$$

was used, in this case to emphasize the excellent agreement of the thick-film device with theory and the data on pellet-type sensors [15].

Figure 7. Reproducibility of the thick-film sensor concept. For comparison, data reported in the literature for a pellet-like sensor [15] were included, as well as the values expected from theory (Eq. 4a, solid line).

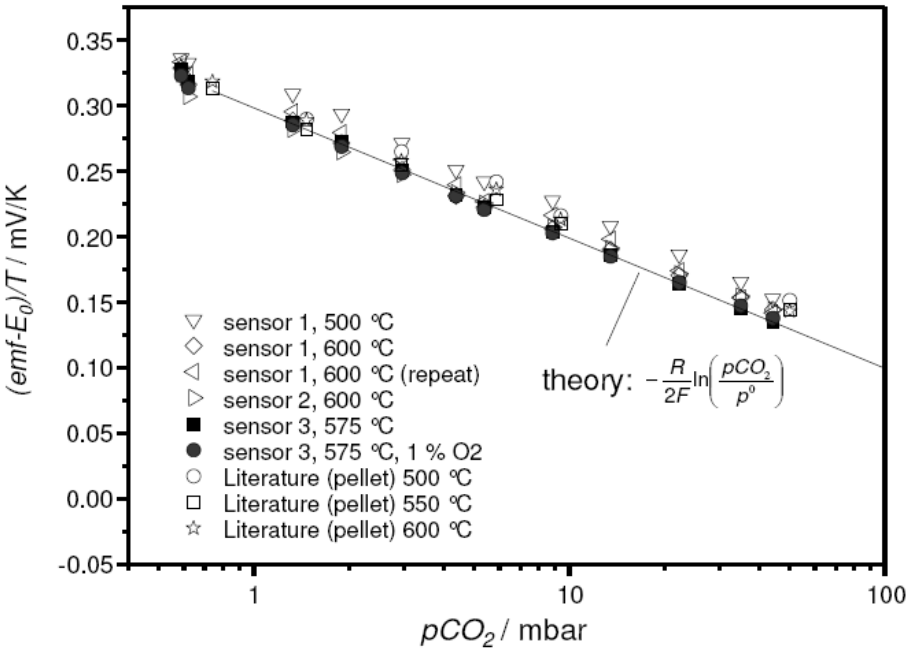

Based on these promising results, actively heated devices with the sodium-poor reference material were prepared. For this purpose, a sensor chip was glued on top of a screen-printed platinum heater using ceramic paste. Silver served as a shielding layer to prevent voltage interferences from the heater. The sensor was then mounted into a corresponding sample holder attached to a voltage source. By monitoring the resistance of the platinum heater after previous calibration, its temperature could be controlled in the range from 100 °C to 700 °C. Again, operating temperatures of 500 °C and 600 °C were chosen.

Figure 8 presents the results of four consecutive measurement cycles conducted on a thick-film sensor with the sodium-poor reference. The temperature of the device was adjusted to 575 °C and exposed to a cold gas stream of 200 sccm/min. The carbon dioxide partial pressure pCO_2 was varied stepwise between 0.4 mbar and 45 mbar. The spikes that occur consistently between the 13.5 mbar and the 9 mbar step are an artifact related to the gas dosage system of the test bench. In order to access low pCO_2 values, the gas dosage is switched to a dilution line and back again to achieve high pCO_2. This switching is accompanied by a pressure surge leading to the observed *emf* spikes. The actively heated sensor presented a stable and reproducible response, which was insensitive to a variation in the oxygen partial pressure from 200 mbar (20 % O_2) to 10 mbar (1 % O_2). As shown in the top part of Figure 8, the sensor characteristics of each measurement cycle coincide. The electron transfer number calculated from the slope of this semilogarithmic plot equaled 1.94. For comparison, the values expected from

theory were included in Figure 8 as a solid line. They were calculated using the Nernst equation (Eq. 4) with the E_0 value estimated from Ref. [15].

Figure 8. *emf* response of a thick-film device with the sodium-poor reference composition, heated to 575 °C by a screen-printed platinum heater. **Bottom part**: *emf* trace. **Top part**: semilogarithmic plot as a function of pCO_2 (values expected from theory (Eq. 4) were included for comparison as solid line). Total gas flow: 200 sccm/min. For details see text.

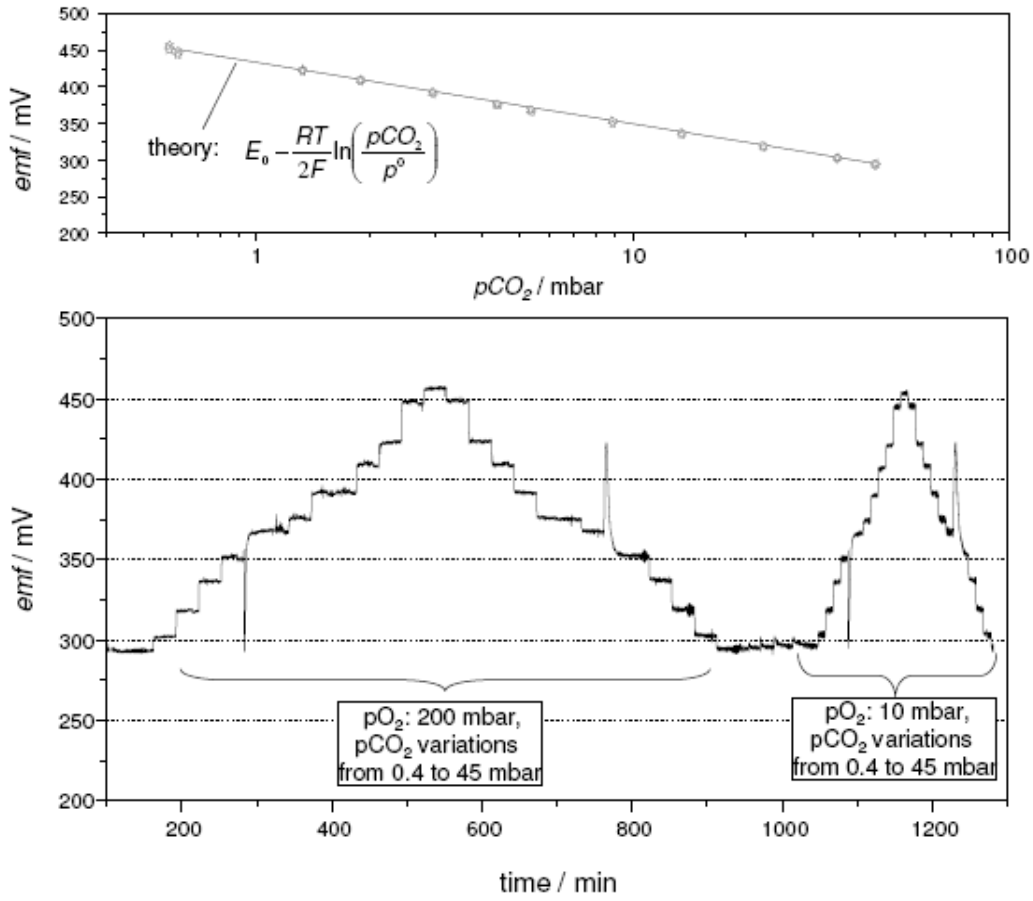

4. Conclusions

The potentiometric sensor concept with an open sodium titanate reference, which had formerly been investigated in a ceramic pellet set-up, was successfully transferred to thick-film technology. After identifying the appropriate reference composition, screen-printed sensor devices were prepared and tested with respect to CO_2 response, reproducibility, and cross-interference of oxygen. For the thick-film sensors using a sodium-poor reference formulation, excellent agreement with the theory was observed. After attaching a screen-printed heater, sensor elements were operated actively in a cold gas stream.

Future work is directed to further miniaturizing the thick film sensor, i.e., in a hot-plate set-up as shown in [19] and [20]. In particular, the direct integration of a heating element on one single chip is envisioned.

References

1. Holzinger, M.; Maier, J.; Sitte, W. Potentiometric detection of complex gases: application to CO_2, *Solid State Ionics* **1997**, *94*, 217-225.
2. Weppner, W. Solid-state electrochemical gas sensors. *Sens. Actuators* **1987**, *12*, 107-119.
3. Kaneyasu, K.; Otsuka, K.; Setoguchi, Y.; Sonoda, S.; Nakahara, T.; Aso, I.; Nakagaichi, N. A carbon dioxide gas sensor based on solid electrolyte for air quality control. *Sens. Actuators B: Chemical* **2000**, *66*, 56-58.
4. Mason, L.W.; Oh, S.; Joseph, J.P. Development and testing of a solid-state CO_2 gas sensor for use in reduced-pressure environments. *Sens. Actuators B: Chemical* **1995**, *24-25*, 407-411.
5. Kida, T.; Shimanoe, K.; Miura, N.; Yamazoe, N. Stability of NASICON-based CO_2 sensor under humid conditions at low temperature. *Sens. Actuators B: Chemical* **2001**, *75*, 179-187.
6. Näfe, H.; Aldinger, F. CO_2 sensor based on a solid state oxygen concentration cell. *Sens. Actuators B: Chemical* **2000**, *69*, 46-50.
7. Alonso-Porta, M.; Kumar, R.V. Use of NASICON/Na_2CO_3 system for measuring CO_2. *Sens. Actuators B: Chemical* **2000**, *71*, 173-178.
8. Obata, K.; Shimanoe, K.; Miura, N.; Yamazoe, N. NASICON devices attached with Li_2CO_3-$BaCO_3$ auxiliary phase for CO_2 sensing under ambient conditions. *J. Mater. Sci*. **2003**, *38*, 4283-4288.
9. Quan, Y.H.B.; Wang, B.; Zhang, C.; Liu, F. Investigation of miniature CO_2 gas sensor based on NASICON. *Russ. J. Electrochem*. **2007**, *43*, 1289-1293.
10. Wang, L.; Kumar, R.V. Thick film CO_2 sensors based on Nasicon solid electrolyte. *Solid State Ionics* **2003**, *158*, 309-315.
11. Kida, T.; Kishi, S.; Yuasa, M.; Shimanoe, K.; Yamazoe, N. Planar NASICON-based CO_2 sensor using BiCuVOx/perovskite-type oxide as a solid-reference electrode. *J. Electrochem. Soc.* **2008**, *155*, J117-J121.
12. Shim, H.B.; Kang, J.H.; Choi, J.W.; Yoo, K.S. Characteristics of thick-film CO_2 sensors based on NASICON with Na_2CO_3-$CaCO_3$ auxiliary phases. *J. Electroceramics* **2006**, *17*, 971-974.
13. Miyachi, Y.; Sakai, G.; Shimanoe, K.; Yamazoe, N. Fabrication of CO_2 sensor using NASICON thick film. *Sens. Actuators B: Chemical* **2003**, *93*, 250-256.
14. Kida, T.; Miyachi, Y.; Shimanoe, K.; Yamazoe, N. NASICON thick film-based CO_2 sensor prepared by a sol-gel method. *Sens. Actuators B: Chemical* **2001**, *80*, 28-32.
15. Holzinger, M.; Maier, J.; Sitte, W. Fast CO_2-selective potentiometric sensor with open reference electrode. *Solid State Ionics* **1996**, *86-88*, 1055-1062.
16. Maier, J.; Holzinger, M.; Sitte, W. Fast potentiometric CO_2 sensors with open reference electrodes. *Solid State lonics* **1994**, *74*, 5-9.
17. Maier, J. Electrochemical sensor principles for redox–active and acid-base–active gases. *Sens. Actuators B: Chemical* **2000**, *65*, 199-203.
18. Sahner, K.; Schönauer, D.; Moos, R.; Matam, M.; Post, M.L. Effect of electrodes and zeolite cover layer on hydrocarbon sensing with p-type perovskite $SrTi_{0.8}Fe_{0.2}O_{3-\delta}$ thick and thin films. *J. Mater. Sci.* **2006**, *41*, 5828-5835.

19. Rettig, F.; Moos, R. Ceramic meso hot-plates for gas sensors. *Sens. Actuators B: Chemical* **2004**, *103*, 91-97.
20. Kita, J.; Rettig, F.; Moos, R.; Drue, K.; Thust, H. Hot plate gas sensors - Are ceramics better? *Int. J. Appl. Ceram. Technol*. **2005**, *2*, 383-389.